Neuron, Volume *98*

Supplemental Information

Complementary Tuning of Na^+ and K^+ Channel Gating Underlies Fast and Energy-Efficient Action Potentials in GABAergic Interneuron Axons

Hua Hu, Fabian C. Roth, David Vandael, and Peter Jonas

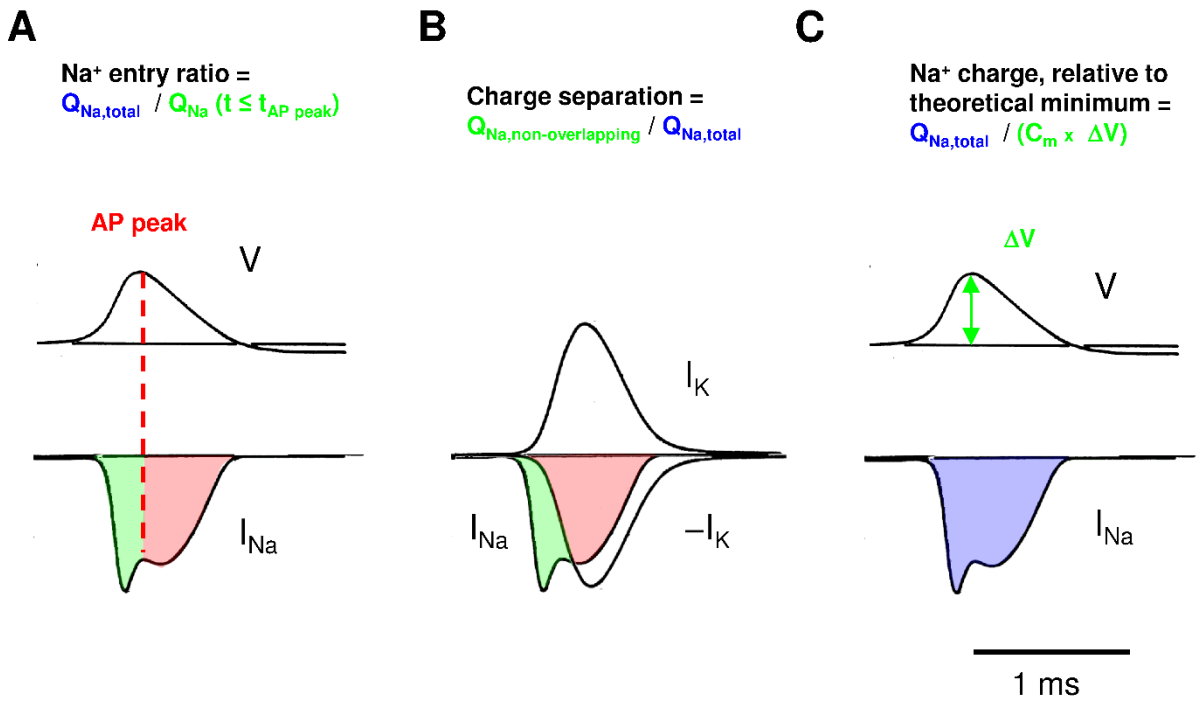

Figure S1. Definition of three different measures of energy efficiency of APs, related to Figures 1–4.

(**A**) Na^+ entry ratio (Hallermann et al., 2012). Vertical red line indicates the time of the peak of the AP. Green, Na^+ charge before AP peak; red, Na^+ charge after AP peak.

(**B**) Na^+-K^+ charge separation (Alle et al., 2009). Green, non-overlapping component; red, overlapping component of Na^+ current.

(**C**) Total Na^+ charge, relative to the theoretical minimum (Alle et al., 2009; Carter and Bean, 2009). Blue, value obtained by integration of Na^+ current. V indicates voltage, I_{Na} and I_K represent sodium and potassium currents during an AP. $-I_K$ depicts inverted potassium current, used to illustrate current overlap. Traces were taken from simulations of propagated APs in squid giant axon (Hodgkin and Huxley, 1952).

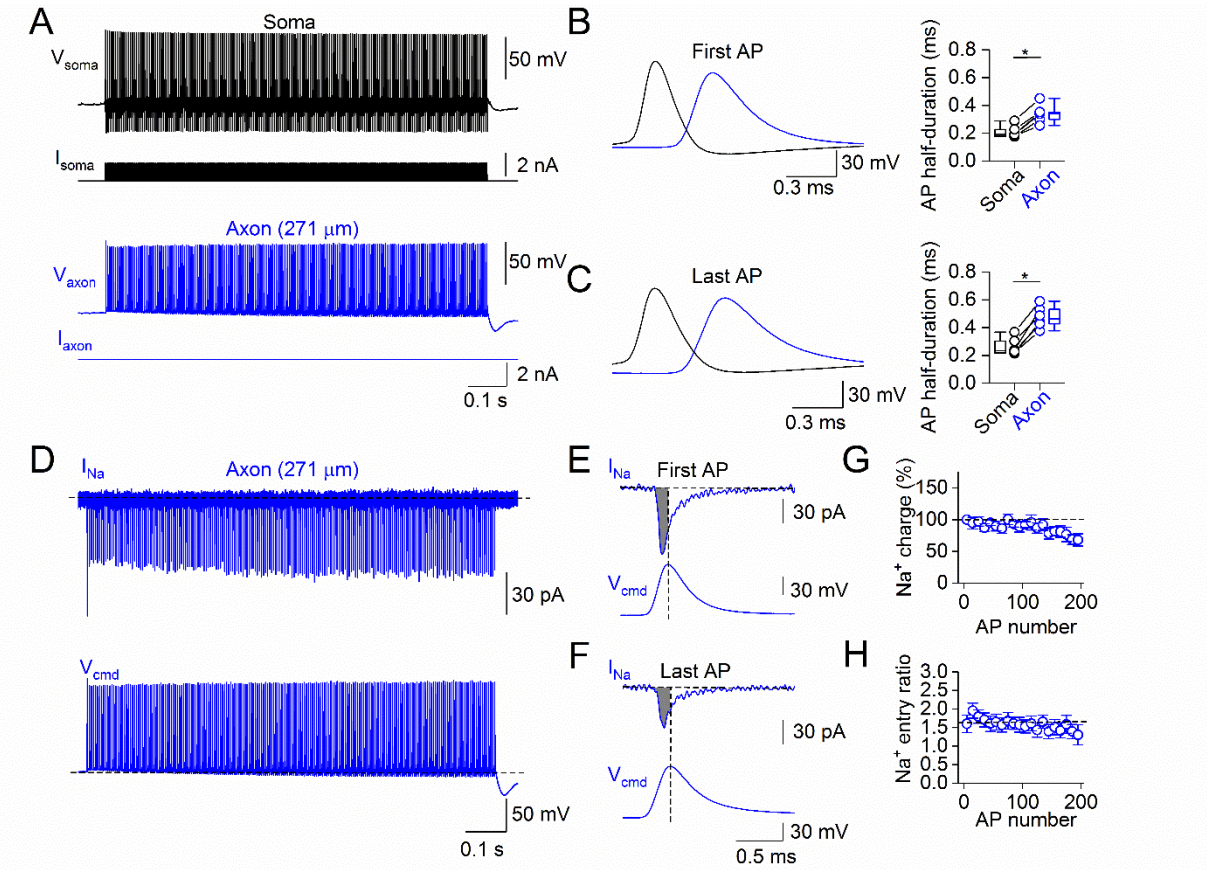

Figure S2. Activity-dependence of Na^+ entry during repetitive high-frequency firing, related to Figures 1 and 2.

(**A**) A simultaneous soma–axon recording from a PV^+-BC during somatic injection of a high-frequency train of short current pulses (200 stimuli at 200 Hz; 2 ms, 1.5 nA). Black traces, somatic voltage and corresponding current; blue traces, axonal voltage and corresponding current (271 µm from the soma).

(**B**) Left, overlay of somatic and axonal membrane potentials during the first AP in the train. Right, summary graph depicts first somatic and axonal AP half-durations in the 200-Hz train. Open circles, data from individual recordings. Somatic and axonal data points from the same experiment were connected by lines. Whiskers in box charts indicate the 5th and 95th percentile of data points, and the box itself indicates median, first quartile, and third quartile of the data points. * indicates P = 0.04

(**C**) Similar to (B), but for the last AP in the 200-Hz train. * indicates P = 0.04.

(**D**) Na^+ current (top) elicited by the 200-Hz AP train waveform (bottom) in the outside-out patch excised from a PV^+-BC axon (271 µm from the soma).

(**E, F**) Na^+ currents (top) elicited by the first (E) and last (F) APs (bottom) in the 200-Hz train shown at expanded scales. Filled gray area represents Na^+ entry before the AP peak.

Data in (A)–(F) are from the same cell.

(**G**) Plot of Na^+ charge transfer during the 200-Hz AP trains against AP number in 6 axonal recordings. Values in (G) normalized to those of the first AP in the train.

(**H**) Plot of Na^+ entry ratio during the 200-Hz AP trains against AP number in 6 axonal recordings. Each data point in (G) and (H) represents the mean value of 10 consecutive APs in the 200-Hz train.

Values in (G) and (H) are presented as mean ± SEM.

Recordings were performed at ~35°C.

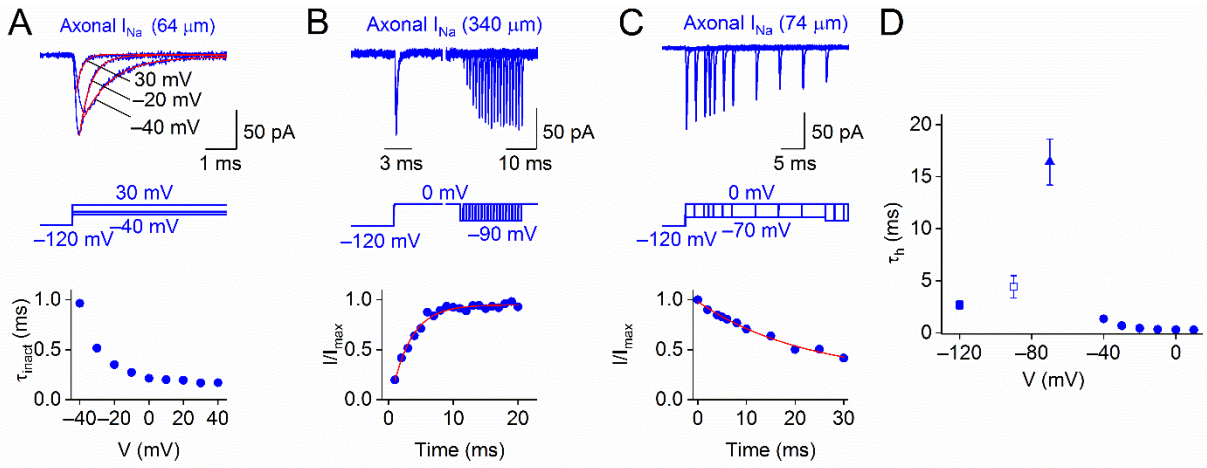

Figure S3. Rapid inactivation kinetics of Na^+ channels in PV^+-BC axons, related to Figures 2–4.

(**A**) Top, Na^+ currents and corresponding voltage pulses in an outside-out patch excised from a PV^+-BC axon (64 µm from the soma). Red lines represent monoexponential functions fit to the decay of the recorded traces. Bottom, plot of Na^+ channel inactivation time constant against voltage in the same recording. Data in (A) are replotted from Figure S6 in Hu and Jonas, 2014.

(**B**) Top, Na^+ currents and corresponding voltage pulses in an outside-out patch excised from a PV^+-BC axon (340 µm from the soma), demonstrating the fast time course of Na^+ current recovery from inactivation at −90 mV. Bottom, plot of Na^+ current peak amplitude against the duration of the interpulse interval at −90 mV in the same recording. The time constant of Na^+ channel recovery from inactivation was obtained by fitting the data points with a monoexponential function with an offset (τ = 3.0 ms, red line).

(**C**) Top, Na^+ currents and corresponding voltage pulses in an outside-out patch excised from a PV^+-BC axon (74 µm from the soma), demonstrating the time course of onset of Na^+ channel inactivation at −70 mV. Bottom, plot of Na^+ current peak amplitude against the duration of the conditioning pulse at −70 mV in the same recording. The time constant of onset of Na^+ channel inactivation was obtained by fitting the data points with a monoexponential function with an offset (τ = 22.5 ms, red line).

(**D**) Time constants of Na^+ current inactivation (filled circles, 11 axonal recordings), onset of inactivation at −70 mV (filled triangle, 7 axonal recordings), recovery from inactivation at −90 mV (open square, 3 axonal recordings) and recovery at −120 mV (filled square, 5 axonal recordings) plotted against voltage. For onset of inactivation at

−70 mV and recovery from inactivation at −90 mV or −120 mV, mean values were obtained by fit of average data, whereas SEM values were obtained from fits of data from individual experiments.

Values are presented as mean ± SEM. Recordings were obtained at ~24°C.

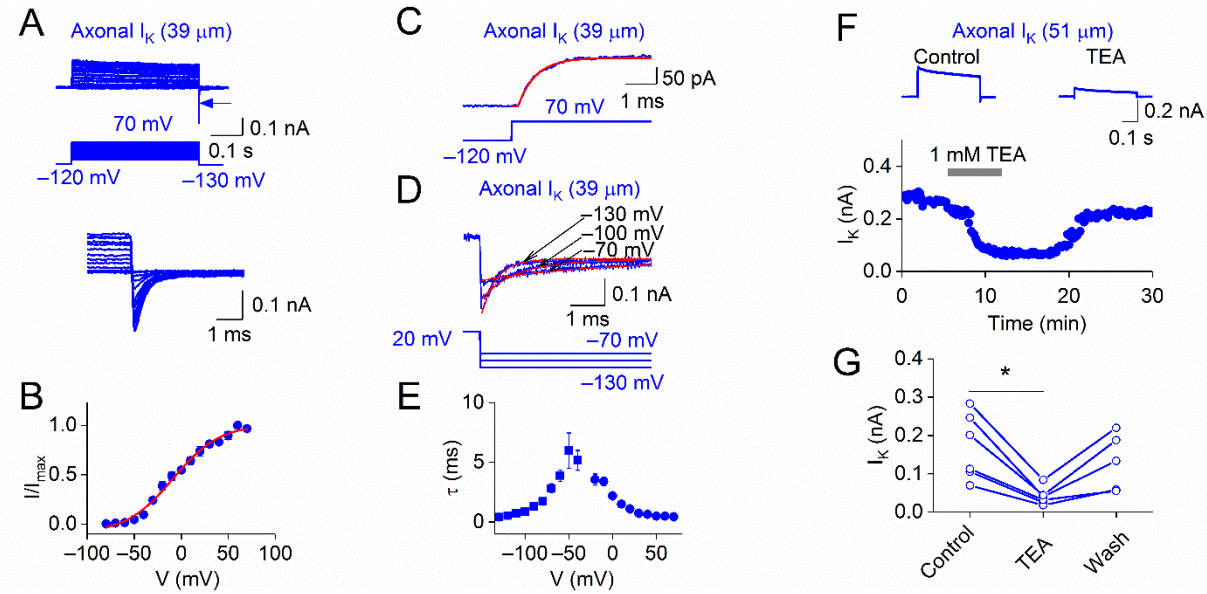

Figure S4. Gating and pharmacological properties of K⁺ channels in PV⁺-BC axons, related to Figures 2–4.

(**A**) Top, K⁺ currents in an outside-out patch excised from a PV⁺-BC axon 39 µm from the soma. The corresponding pulse protocol with increasing test pulse amplitude is shown in the center. Arrow indicates K⁺ tail currents at −130 mV, which were plotted at expanded scales at the bottom.

(**B**) Steady-state K⁺ current activation curve in PV⁺-BC axons. K⁺ current amplitudes were measured from tail currents at −130 mV and normalized to the maximal value in each experiment. Red line represents a Boltzmann function fit to the data points (5 axonal recordings).

(**C**) Top, onset of K⁺ current and corresponding voltage pulses in an outside-out patch excised from a PV⁺-BC axon (39 µm from the soma). Red lines represent a monoexponential function with delay fit to the current trace.

(**D**) K⁺ tail currents and the corresponding deactivation pulse protocol in an outside-out patch excised from a PV⁺-BC axon (39 µm from the soma). Red lines represent monoexponential functions fit to the tail currents. Data in (A), (C), and (D) were obtained from the same recording.

(**E**) Time constants of K⁺ current activation (filled circles, 5 axonal recordings) and deactivation (filled squares, 5 axon recordings) plotted against voltage.

(**F**) Top, K^+ currents in an axonal membrane patch excised 51 µm from the soma before and during bath application of 1 mM TEA. Bottom, steady-state K^+ current amplitude plotted against experimental time during the TEA application.

(**G**) Summary plot of steady-state K^+ current amplitude before, during, and after the application of TEA in 6 axonal patches. Data from the same experiment were connected by lines. * indicates P = 0.04.

Values in (B) and (E) are presented as mean ± SEM. Recordings were obtained at ~24°C.

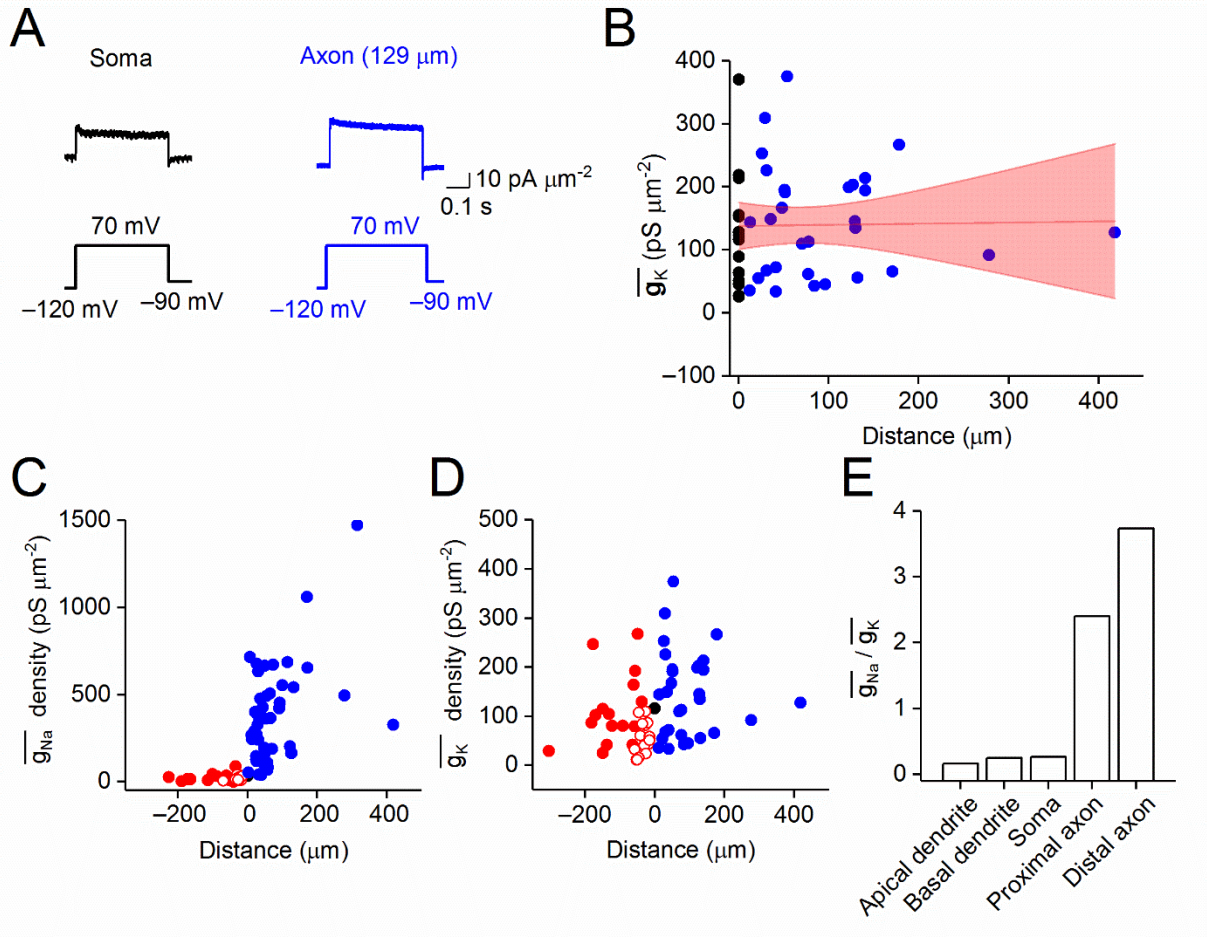

Figure S5. A steep subcellular gradient of Na^+ to K^+ conductance ratio in PV^+-BCs, related to Figures 2 and 3.

(**A**) Density of K^+ current in outside-out patches from the soma and the axon (129 µm from the soma). Black traces, somatic current density and corresponding voltage; blue traces, axonal current density and corresponding voltage. The current density was obtained dividing the current by the estimated patch area.

(**B**) K^+ conductance density plotted against distance from the soma. Black circles, data from 11 somatic recordings; blue circles, data from 30 axonal recordings. Data were fit with a linear function (red line, Spearman ρ = 0.42, P = 0.13). Red area represents 95% confidence interval.

(**C**) Summary plot of distance dependence of subcellular $\overline{g_{Na}}$ density in PV^+-BCs. Filled red circles, 15 apical dendritic patches; open red circles, 9 basal dendritic patches; filled black circle, median of 41 somatic patches; filled blue circles, 37 proximal (< 100 µm) and 11 distal (≥ 100 µm) axonal patches. Axonal data points were taken from Hu and Jonas, 2014.

(**D**) Summary plot of distance dependence of subcellular $\overline{g_K}$ density in PV$^+$-BCs. Filled red circles, 17 apical dendritic patches; open red circles, 14 basal dendritic patches; filled black circle, median of 11 somatic patches; filled blue circles, 19 proximal (< 100 µm) and 11 distal (≥ 100 µm) axonal patches. In (C) and (D), positive distances indicate axon, while negative distances represent dendrites.

(**E**) A steep subcellular gradient of Na^+ to K^+ conductance ratio in PV$^+$-BCs. To calculate the Na^+ to K^+ conductance ratio in each subcellular compartment, the median $\overline{g_{Na}}$ density was divided by the corresponding median $\overline{g_K}$ density.

Recordings were obtained at ~24°C.

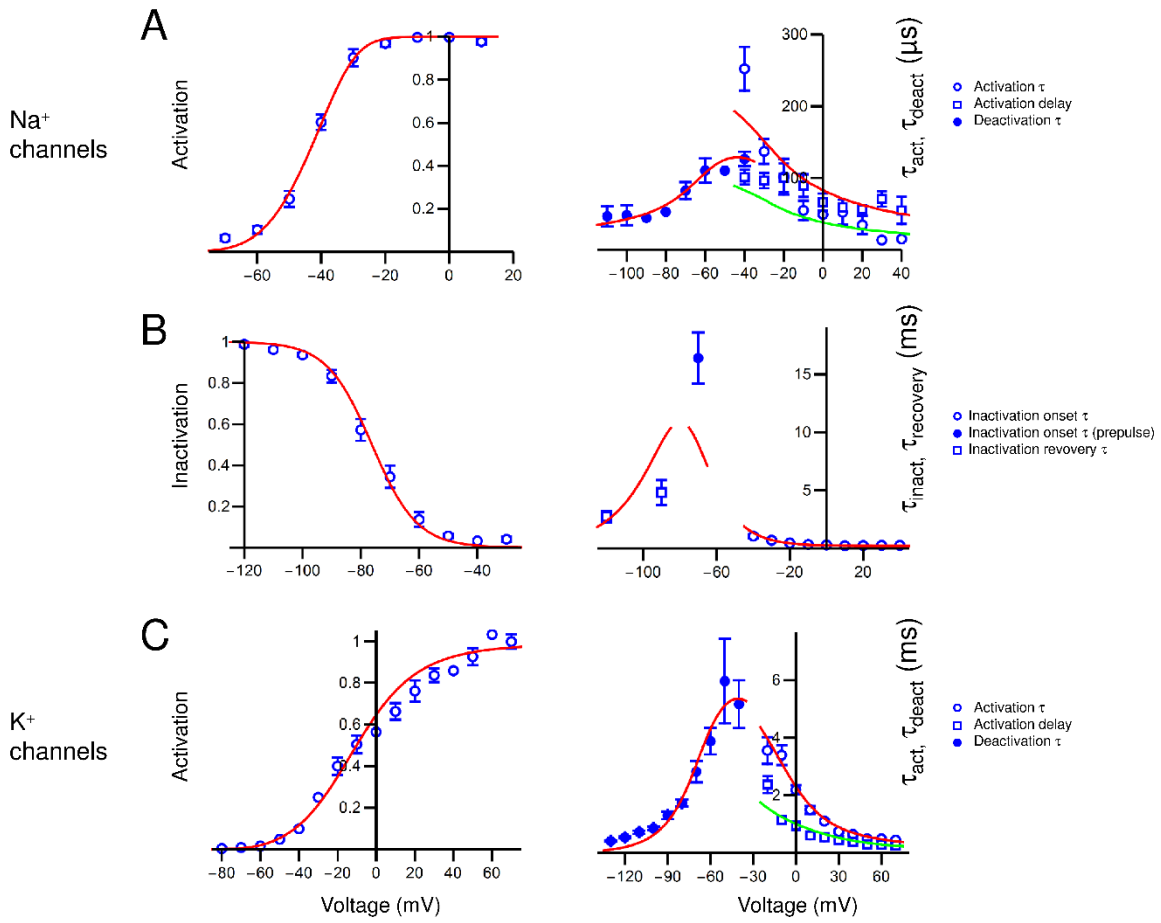

Figure S6. Experimentally constrained models of Na^+ and K^+ channels in PV^+-BC axons, related to Figures 2–4.

(**A**) Modeling of Na^+ channel activation. Left, Na^+ channel activation curve; right, activation time constants, delay, and deactivation time constants.

(**B**) Modeling of Na^+ channel inactivation. Left, steady-state inactivation curve; right, time constants of inactivation onset and recovery.

(**C**) Modeling of K^+ channel activation. Left, K^+ channel activation curve; right, activation time constants, delay, and deactivation time constants. Continuous curves in left plots indicate model predictions for activation and inactivation curves. Continuous curves in right plots indicate model predictions for time constants (red) and delay (green). For model parameters, see Table S5.

Values are presented as mean ± SEM.

Table S1. Comparison of energy efficiency measures in PV^+-BC axons with those in other types of axons, related to Figures 1–5.

Axon	Na^+ entry ratio	Charge separation	Total Na^+ charge / theoretical minimum	Total ATP consumption AP^{-1}	Reference
PV^+-BC axon	1.60 ± 0.13	0.59 ± 0.06	1.46 ± 0.27	107 ± 30 × 10^6	This paper
Squid axon			~4		Hodgkin, 1975; Sengupta et al., 2010
Crab axon			3.43		Sengupta et al., 2010
Mossy fiber axon		0.80 ± 0.02	1.26		Alle et al., 2009
Layer 5 pyramidal neuron axon	2.28 ± 0.16; 1.8 ± 0.2	0.63 ± 0.03		400–800 × 10^6	Hallermann et al., 2012

Table S2. Properties of somatic and axonal APs in PV^+-BCs during a 1-s high-frequency train at physiological temperature, related to Figure 1.

First AP				
	Peak amplitude	**Half-duration**	**Maximal rise slope**	**Maximal decay slope**
Soma (n = 41)	79.0 ± 1.8 mV	0.22 ± 0.01 ms	705 ± 30 V s^{-1}	388 ± 20 V s^{-1}
Proximal axon [a] (n = 22)	88.7 ± 3.6 mV	0.26 ± 0.01 ms	1014 ± 72 V s^{-1}	352 ± 20 V s^{-1}
Distal axon [a] (n = 14)	82.9 ± 2.4 mV	0.32 ± 0.03 ms	620 ± 63 V s^{-1}	257 ± 26 V s^{-1}
Entire axon (n = 41)	86.4 ± 2.2 mV	0.29 ± 0.02 ms	784 ± 51 V s^{-1}	302 ± 17 V s^{-1}
Last AP				
	Peak amplitude	**Half-duration**	**Maximal rise slope**	**Maximal decay slope**
Soma (n = 36)	57.0 ± 2.7 mV	0.37 ± 0.03 ms	336 ± 36 V s^{-1}	171 ± 21 V s^{-1}
Proximal axon [a] (n = 20)	50.1 ± 5.0 mV	0.53 ± 0.03 ms	283 ± 54 V s^{-1}	119 ± 18 V s^{-1}
Distal axon [a] (n = 12)	62.8 ± 4.4 mV	0.53 ± 0.08 ms	338 ± 40 V s^{-1}	117 ± 13 V s^{-1}
Entire axon (n = 36)	60.0 ± 3.2 mV	0.55 ± 0.03 ms	338 ± 34 V s^{-1}	110 ± 11 V s^{-1}

Recordings were performed at ~35˚C.

Values in Table S2 are presented as median ± SEM.

[a] Boundary between proximal and distal compartment was set at a distance of 100 µm from axon origin.

Table S3. Gating properties and density of Na^+ conductance in PV^+-BC axons, related to Figures 3, 4 and 5.

	Activation	**Deactivation**	**Inactivation**	**Inactivation onset / recovery (prepulses)**
Midpoint potential	−40.1 ± 1.1 mV (n = 14) [a]		−76.5 ± 1.6 mV (n = 13) [a]	
Slope factor	7.4 ± 0.6 mV (n = 14) [a]		7.8 ± 0.2 mV (n = 13) [a]	
τ	230 ± 17 µs at −40 mV (n = 4) [a]	126 ± 8 µs at −40 mV (n = 7) [a]	1.50 ± 0.14 ms at −40 mV (n = 11) [a]	
τ	61 ± 6 µs at 0 mV (n = 4) [a]	46 ± 9 µs at −110 mV (n = 7) [a]	319 ± 21 µs at 0 mV (n = 11) [a]	
τ				16.4 ± 2.2 ms at −70 mV (n = 7)
τ				4.42 ± 1.07 ms at −90 mV (n = 3)
τ				2.70 ± 0.38 ms at −120 mV (n = 5)
$\overline{g_{Na}}$	271.1 ± 32.7 pS µm^{-2} (n = 37) in proximal axon [a] 542.1 ± 120.8 pS µm^{-2} (n = 11) in distal axon [a]			

[a] Median and SEM values were determined from Hu and Jonas, 2014.

Values in Table S3 are presented as median ± SEM.

Table S4. Gating properties and density of K^+ conductance in PV^+-BC axons, related to Figures 3 and 5.

	Activation	**Deactivation**
Midpoint potential	−4.8 ± 5.3 mV (n = 5)	
Slope factor	22.9 ± 3.9 mV (n = 5)	
τ	449 ± 27 µs at 70 mV (n = 5)	4.11 ± 0.83 ms at −40 mV (n = 5)
τ	3.06 ± 0.47 ms at −20 mV (n = 5)	403 ± 23 µs at −130 mV (n = 5)
$\overline{g_K}$	113.1 ± 22.7 pS µm^{-2} in proximal axon (n = 19) 145.1 ± 20.2 pS µm^{-2} in distal axon (n = 11)	

Values in Table S4 are presented as median ± SEM.

Table S5. Hodgkin-Huxley-type model of Na^+ and K^+ channels gating in PV^+-BC axons, related to Figures 5.

Na^+ channels	α_m	β_m	α_h	β_h
A	0.2567 ms^{-1}	0.1133 ms^{-1}	0.00105 ms^{-1}	4.827 ms^{-1}
B	60.84 mV	30.253 mV	-	18.646 mV
C	9.722 mV	2.848 mV	20.000 mV [a]	12.452 mV
K^+ channels	α_n	β_n	$\alpha_{n'}$	$\beta_{n'}$
A	0.0610 ms^{-1}	0.001504 ms^{-1}	0.0993 ms^{-1}	0.1379 ms^{-1}
B	−29.991 mV	-	−33.720 mV	-
C	27.502 mV	17.177 mV	12.742 mV	500.000 mV [a]

$\alpha_m(V) = A\,[-(V+B)] / \{\mathrm{Exp}[-(V+B) / C] - 1\}$ (Eq. 1a)

$\beta_m(V) = A\,(V+B) / \{\mathrm{Exp}[(V+B) / C] - 1\}$ (Eq. 1b)

$\alpha_h(V) = A\,\mathrm{Exp}(-V / C)$ (Eq. 2a)

$\beta_h(V) = A / \{\mathrm{Exp}[-(V+B) / C] + 1\}$ (Eq. 2b)

$\alpha_n(V) = A\,[-(V+B)] / \{\mathrm{Exp}[-(V+B) / C] - 1\}$ (Eq. 3a)

$\beta_n(V) = A\,\mathrm{Exp}(-V / C)$ (Eq. 3b)

$\alpha_n'(V) = A\,[-(V+B)] / \{\mathrm{Exp}[-(V+B) / C] - 1\}$ (Eq. 4a)

$\beta_n'(V) = A\,\mathrm{Exp}(-V / C)$ (Eq. 4b)

[a] At limit of parameter range

Table S6. Parameters of single-compartment model, related to Figure 5.

Parameter	Value	Reference
C_m	9 fF µm^{-2} (0.9 µF cm^{-2})	Nörenberg et al., 2010
g_L	1 pS µm^{-2} (0.1 mS cm^{-2})	
$\overline{g_{Na}}$	500 pS µm^{-2}	Hu and Jonas, 2014
$\overline{g_K}$	150 pS µm^{-2}	Hu et al., 2010; this paper
V_{Na}	+55 mV	
V_K	−90 mV	
V_L	−65 mV	
V_{rest}	−65 mV	
Q_{10} (m, h, and n or n')	2.2, 2.9, 3.0	Schwarz and Eikhof, 1987; Frankenhaeuser and Moore, 1963

Rates (Eq. 1 – 4) were temperature- and offset-corrected before use in simulations (for details, see METHOD DETAILS).

Table S7. Parameters and predictions of detailed cable model, related to Figure 5.

Parameter	Value	Reference
C_m	9 fF µm^{-2} (0.9 µF cm^{-2})	Nörenberg et al., 2010
g_L	1 pS µm^{-2} (0.1 mS cm^{-2})	
R_i	1.7 MΩ µm (170 Ω cm)	Nörenberg et al., 2010
$\overline{g_{Na}}$ (axon)	500 pS µm^{-2}	Hu and Jonas, 2014
$\overline{g_{Na}}$ (soma)	200 pS µm^{-2}	
$\overline{g_{Na}}$ (dendrites)	50 pS µm^{-2}	Hu et al., 2010
$\overline{g_K}$	300 pS µm^{-2}	Hu et al., 2010; this paper
V_{Na}	+55 mV	
V_K	−90 mV	
V_L	−70 mV	
V_{rest}	−70 mV	
Q_{10} (m, h, and n or n')	2.2, 2.9, 3.0	Schwarz and Eikhof, 1987; Frankenhaeuser and Moore, 1963

Rates (Eq. 1 – 4) were temperature- and offset-corrected before use in simulations (for details, see METHOD DETAILS).

Predictions of the model

AP properties				
Compartment	**Peak amplitude**	**Half-duration**	**Maximal rise slope**	**Maximal decay slope**
Soma	81.3 ± 1.5 mV	0.671 ± 0.021 ms	206 ± 15 V s^{-1}	134 ± 4 V s^{-1}
Axon	84.2 ± 4.7 mV	0.400 ± 0.069 ms	475 ± 25 V s^{-1}	240 ± 12 V s^{-1}
Apical dendrite	19.6 ± 2.7 mV	0.667 ± 0.042 ms	59 ± 7 V s^{-1}	49 ± 7 V s^{-1}
Basal dendrite	41.3 ± 8.8 mV	0.626 ± 0.036 ms	104 ± 24 V s^{-1}	101 ± 23 V s^{-1}

Values in Table S7 are presented as median ± SEM.